The Journal of Chemical Physics

Suppression and enhancement of van der Waals interactions

Minhaeng Cho and Robert J. Silbey

Citation: J. Chem. Phys. **104**, 8730 (1996); doi: 10.1063/1.471562
View online: http://dx.doi.org/10.1063/1.471562
View Table of Contents: http://jcp.aip.org/resource/1/JCPSA6/v104/i21
Published by the American Institute of Physics.

Suppression and enhancement of van der Waals interactions

Minhaeng Cho[a] and Robert J. Silbey
Department of Chemistry, Massachusetts Institute of Technology, Cambridge, Massachusetts 02139

(Received 18 January 1996; accepted 12 February 1996)

The van der Waals interaction of a pair of anisotropic molecules near planar dielectric surfaces is studied by using the linear response formalism. The spatial correlation function (Green function) of the vacuum electric field in the presence of dielectric surfaces is obtained by using suitable Fresnel mode functions of the quantized electric field. In the short-distance limit, it is observed that the long-range interaction potential is significantly modified by the dielectric surfaces and strongly depends on the geometry of the two molecules near dielectric surfaces. When the two molecules are anisotropic, depending on the molecular alignments with respect to the surfaces, the van der Waals interaction is enhanced or suppressed by the existence of the surfaces. When the two molecules are in between two dielectric surfaces, the overall magnitude of the van der Waals interaction is suppressed in comparison to that in the free space because the vacuum electromagnetic field intensity is reduced by the transmissivities that are generally less than unity. © *1996 American Institute of Physics.* [S0021-9606(96)00219-8]

I. INTRODUCTION

Boundary effects on various quantum phenomena, such as level shifts of an atom in various types of cavities, enhancement or suppression of spontaneous emission rate, excitation transfer etc., are of current interests both theoretically and experimentally.[1] The modifications by the boundary conditions are the manifestation of the changes in mode structures of electromagnetic fields near boundaries. For example, the spontaneous emission rate of an excited atom near a dielectric surface can be enhanced or suppressed depending on the distance from the surface.[1–3] Based on the Fermi Golden rule, the spontaneous emission rate is proportional to the mean square fluctuation amplitude of the quantum vacuum field.[4–6] In the vicinity of a dielectric surface,[7] the spatial variation of the field fluctuation amplitude differs from that of the free space, which in turn cause modulations of spontaneous emission rate as a function of distance from the surface. In this paper, we shall show how these changes in modal structures near planar surfaces modify the van der Waals interaction between two polarizable molecules.

It was perhaps MacLachlan[8] who first showed that the van der Waals interaction between two neutral polarizable molecules can be significantly altered by the existence of the dielectric surface compared to that of the free space. He showed that the van der Waals interaction potential of a pair of molecules in the vicinity of a dielectric surface depends on the detailed geometry. If the two molecules are located side by side parallel to the dielectric surface, the intermolecular interaction decreases in comparison to that in the free space. In contrast, when one is on top of the other, the interaction potential increases. In case when the anisotropy of the molecular polarizability is large, this boundary effect, induced by a single dielectric surface, on the van der Waals interaction of a pair of molecules can be very large so that the van der Waals interaction could be suppressed or enhanced dramatically. Although this case was theoretically studied by Imura and Okano,[9] the clear physical interpretations and implications of these results were not fully explored in their paper.

In this paper, we focus on the more general situation when two molecules are located in a planar microcavity (see Fig. 1). Particularly, the distance between the two surfaces is much shorter than the most important wavelength of the system, that is, the wavelength of the optical transition frequency of the molecules or dielectric media. Noting that usually the optical transition wavelength is order of hundreds of nanometer, the short distance limit we shall consider is the case when both the intermolecular distance and intersurface distance are smaller than this length scale. If a pair of molecules are located in a planar microcavity (Fabry–Perot cavity), one can expect that the van der Waals interaction is similarly but more strongly modified by the two planar dielectric surfaces, though there are distinctive differences in modal structures in comparison to the case of a single surface. A related problem, the properties of liquid confined by two dielectric surfaces, has been extensively studied by measuring normal and shear forces between the two surfaces as a function of distance between the two surfaces.[10–12] This case is found to be very important in the surface sciences of liquid lubricants, adhesion and wear properties,[13] wetting and dewetting of surfaces,[14] liquid films,[15] etc. Despite of the extensive theoretical studies using Lifshitz's theory[16] and molecular dynamics simulations as well as experimental studies, fundamental aspect of the intermolecular interaction between molecules in a plane-confined geometry has not been studied.

In this paper, we shall focus on the van der Waals interaction between two nonpolar molecules when they are in close proximity to the surfaces, treating the surfaces in a macroscopic manner. There exist however numerous effects

[a]Present address: Department of Chemistry, Korea University, Seoul, Korea.

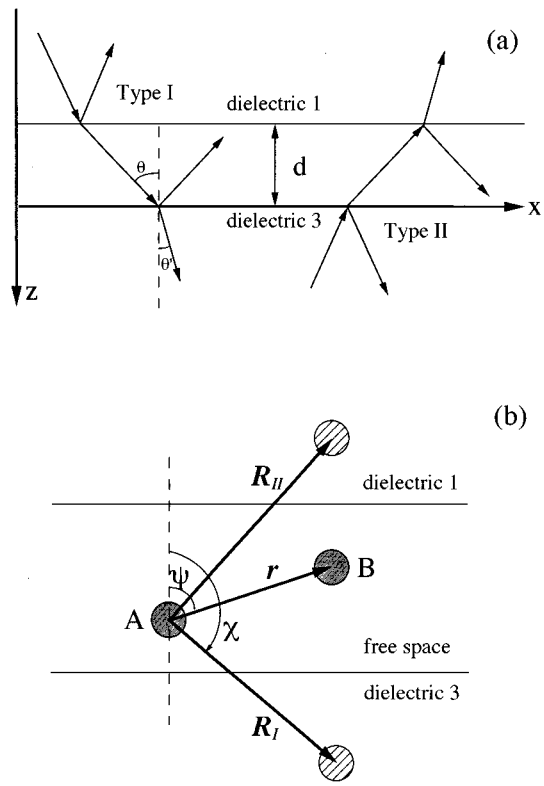

FIG. 1. (a) Two types of modes are shown. Type I modes are associated with the incident modes propagating downward from the dielectric 1 to the interface between the dielectric 1 and the free space, whereas type II modes are associated with the incident modes propagating upward from the dielectric 3 to the interface between the dielectric 3 and the free space. (b) Detailed geometry of the two molecules with respect to the two surfaces are drawn. Two close circles represent the two real molecules in the free space region, whereas the two circles in the dielectric media are pictorial representations of the image molecules of the B-molecule.

that cannot be taken into account by using the macroscopic picture of a solid surface with the phenomenological Maxwell's equations. For example, the nonlocality of the dielectric function near a surface[17–22] may play a crucial role when the distance between the molecules and a surface is order of that between atoms of the solid. Second, the surface can induce a permanent dipole moment by distorting the ground state wave function of the molecule.[17] The magnitude of the induced permanent dipole moment increases as the molecule approaches the surface. Besides of the two complications mentioned above, there exist various mechanisms causing deviations from the van der Waals interaction. In order to remedy the effect of the nonlocality of the dielectric function, Zaremba and Kohn[23] used the jellium model as an approximate microscopic model for a metal surface. They showed, when studying the interaction of a single atom with a metal surface, that the reference (dynamical image) plane position has to be calculated by taking into account the microscopic nature of the metal surface. Thus the effective distance between the molecule and the surface differs from the distance between the molecule and the jellium surface. However, the basic theories developed by Lifshitz are still appropriate in describing key aspects of physisorption and the role of the dielectric surface. Thus, although the results given in this paper will suffer from the lack of a realistic quantum description of the solid surface, they should be useful in understanding fundamental aspects of the boundary effects and in developing proper intermolecular potential functions used in molecular dynamics simulation studies.

This paper is organized as follows. In Sec. II, the effective Hamiltonian of nonpolar polarizable molecules is discussed. The van der Waals interaction between general anisotropic molecules in a planar cavity is considered in Sec. III. Two limiting cases of a single dielectric surface and two dielectric surfaces are discussed in Secs. IV and V, respectively. Finally we summarize the results in Sec. VI.

II. EFFECTIVE INTERACTION HAMILTONIAN

The usual minimal coupling Hamiltonian[24] contains two interaction terms that are linearly and quadratically proportional to the vector potential of the quantized field. By using the Power–Zienau–Wooley transformation,[24–26] one can obtain the multipolar Hamiltonian,

$$H = H_{\mathrm{mol}} + H_F + H_{\mathrm{I}}. \tag{1}$$

The molecular Hamiltonian is, in the second quantized form,

$$H_{\mathrm{mol}} = \sum_m \sum_{\xi(m)} \hbar \Omega_{m\xi} \hat{B}^+_{m\xi} \hat{B}_{m\xi} + \sum_m 2\pi \int d\mathbf{r} |\hat{P}^{\perp}_m(\mathbf{r})|^2. \tag{2}$$

The subscripts m and ζ denote the mth molecule and ζth state of the mth molecule, respectively. $\Omega_{m\zeta}$ is the transition frequency between the ground state $|g(m)\rangle$ and the ζth state $|\xi(m)\rangle$. $\tilde{B}^+_{m\xi}$ and $\hat{B}_{m\xi}$ are transition operators defined by $\hat{B}^+_{m\xi} = |\xi(m)\rangle\langle g(m)|$ and $\hat{B}_{m\xi} = |g(m)\rangle\langle \xi(m)|$, respectively. The transition operators obey the usual commutation relations,

$$[\hat{B}_{m\xi}, \hat{B}^+_{m'\xi'}] = (1 - 2\hat{B}^+_{m\xi}\hat{B}_{m\xi})\delta_{mm'}\delta_{\xi\xi'}. \tag{3}$$

We assumed that the overlap between molecules is ignored. One of the notable difference of the multipolar Hamiltonian from the minimal coupling form is that the intermolecular interaction in the multipolar form is purely determined by the retarded exchange of the virtual transverse photons, whereas the minimal coupling Hamiltonian contains additional instantaneous intermolecular interaction terms.[25,26]

The quantized field Hamiltonian is as usual,[4]

$$H_F = \sum_{k\lambda} \hbar \omega_k (\hat{a}^+_{k\lambda} \hat{a}_{k\lambda} + 1/2), \tag{4}$$

where the photon creation and annihilation operators are denoted by $\hat{a}^+_{k\lambda}$ and $\hat{a}_{k\lambda}$. The interaction Hamiltonian H_{I} in Eq. (1) is

$$H_{\mathrm{I}} = -\int d\mathbf{r} \hat{P}(\mathbf{r}) \cdot \hat{D}(\mathbf{r}). \tag{5}$$

Here the polarization operator, that is associated with the transitions between states of a given molecule, is defined as

$$\hat{P}(\mathbf{r})=\sum_m \hat{\mu}_m \delta(\mathbf{r}-\mathbf{R}_m), \tag{6}$$

where the dipole operator $\hat{\mu}_m$ is

$$\hat{\mu}_m=\sum_{\xi(m)} \overline{\mu_{m\xi}}(\hat{B}_{m\xi}+\hat{B}^+_{m\xi}). \tag{7}$$

$\overline{\mu_{m\xi}}$ is the electric dipole transition matrix element. $\hat{D}(\mathbf{r})$ in the interaction Hamiltonian is the *transverse* displacement field operator, that is the conjugate momentum of the vector potential in the multipolar Hamiltonian,

$$\hat{D}(\mathbf{r})=i\sum_{k\lambda}\left(\frac{2\pi\hbar\omega_k}{V}\right)^{1/2}\{\mathbf{f}_{k\lambda}(\mathbf{r})\hat{a}_{k\lambda}-\mathbf{f}^*_{k\lambda}(\mathbf{r})\hat{a}^+_{k\lambda}\}, \tag{8}$$

and the vector potential is

$$\hat{A}(\mathbf{r})=\sum_{k\lambda}\left(\frac{2\pi\hbar c^2}{V\omega_k}\right)^{1/2}\{\mathbf{f}_{k\lambda}(\mathbf{r})\hat{a}_{k\lambda}+\mathbf{f}^*_{k\lambda}(\mathbf{r})\hat{a}^+_{k\lambda}\}. \tag{9}$$

$\mathbf{f}_{k\lambda}(\mathbf{r})$ are the normalized mode functions satisfying the corresponding Helmholtz equations with the proper boundary conditions.[5]

The interactions between nonpolar polarizable molecules can be described by the second-order or fourth-order perturbation theories depending on the situation. For example, the attractive interaction between a molecule and a dielectric wall is a second-order problem, i.e., quadratic Stark shift,[27,28] that is, the interaction potential is linearly proportional to the molecular polarizability. The interaction of a pair of molecules can be, as shown by London,[29] obtained by using the fourth-order perturbation theory, where the energy shift is proportional to both polarizabilities of the two molecules. Therefore we find that it is useful to derive an effective Hamiltonian by eliminating a one-photon vertex in the Feynman diagrams.[26] By using the Heisenberg equations of motion of the transition operators and introducing the Weisskopf–Wigner approximation (Adiabatic approximation),[30] the effective interaction Hamiltonian can be obtained as

$$H_1^{\text{eff}}=-\sum_m\left[\sum_{k\lambda}\tilde{\alpha}_m(\omega_k):\hat{D}_{k\lambda}(\mathbf{R}_m)\right]\hat{D}(\mathbf{R}_m), \tag{10}$$

where the term in the square bracket in Eq. (10) is the effective induced dipole operator and the molecular polarizability operators are defined as

$$\tilde{\alpha}_m(\omega_k)=\frac{1}{\hbar}\sum_{\xi(m)}[1-\hat{W}_{m\xi}(0)]\overline{\mu_{m\xi}}\,\overline{\mu_{m\xi}}\left(\frac{2\Omega_{m\xi}}{\Omega^2_{m\xi}-\omega_k^2}\right), \tag{11}$$

$\hat{W}_{m\xi}$ is the population operator, $\hat{W}_{m\xi}=2\hat{B}^+_{m\xi}\hat{B}_{m\xi}$. The spontaneous emission contribution to the effective dipole operator was neglected, since we focus on the molecular interaction between two molecules in the ground states. As expected, the effective interaction Hamiltonian given above involves two photon processes. A vacuum field with wave vector $\mathbf{k}$ and polarization direction λ creates an induced dipole at the center of the mth molecule, and in turn this induced dipole interacts with vacuum field at the same position. We shall use a second-order perturbation theory with respect to this effective interaction Hamiltonian to obtain the interaction potential of a pair of nonpolar polarizable molecules.

III. VAN DER WAALS INTERACTION

The van der Waals interaction of a pair of molecules has been a subject of extensive studies since the seminal paper of London.[29] Recently Power and Thirunamachandran[31] showed that the van der Waals–Casimir interaction can be calculated by considering two induced dipoles at the centers of the two molecules and then the two induced dipoles interact through the well-known retarded dipole–dipole interaction tensor obtained by McLone and Power.[32] For a pair of molecules A and B, the interaction energy is thus given by the vacuum expectation value,

$$\Delta E=\sum_{k\lambda}\langle\hat{\mu}^{\text{eff}}_{\text{A}}(\mathbf{k},\lambda)\cdot\tilde{V}(k)\cdot\hat{\mu}^{\text{eff}}_{\text{B}}(\mathbf{k},\lambda)\rangle_{\text{vac}}, \tag{12}$$

where the *effective* induced dipole operators are defined as

$$\hat{\mu}^{\text{eff}}_m(\mathbf{k},\lambda)=\tilde{\alpha}_m(\omega_k)\cdot D_{k\lambda}(\mathbf{R}_m). \tag{13}$$

This result, Eq. (12), can also be obtained by using the second-order perturbation theory with respect to the effective interaction Hamiltonian given in Eq. (10). Inserting the displacement field operator given in terms of mode functions in Eq. (8) into Eqs. (12) and (13) gives

$$\Delta E=-\frac{\hbar c}{\pi}\int_0^\infty dk\ \text{Tr}[\tilde{\alpha}_{\text{A}}(\omega_k)\tilde{V}(k)\tilde{\alpha}_{\text{B}}(\omega_k)\tilde{F}^+(k)], \tag{14}$$

where the dipole–dipole interaction tensor $\tilde{V}(k)$ and its Hilbert transform, $\tilde{F}(k)$, can be written in terms of classical mode functions

$$\tilde{F}(k)\equiv-k^3\ \text{Re}\left[\frac{1}{4\pi}\int d\Omega\sum_\lambda f_{k\lambda}(\mathbf{R}_{\text{A}})\mathbf{f}^*_{k\lambda}(\mathbf{R}_{\text{B}})\right],$$

$$\tilde{V}(k)\equiv\frac{4\pi}{V}\ \text{Re}\sum_{k'\lambda'}\frac{k'^2}{k^2-k'^2}f_{k'\lambda'}(\mathbf{R}_{\text{A}})\mathbf{f}^*_{k'\lambda'}(\mathbf{R}_{\text{B}})$$

$$=\frac{2}{\pi}\int_0^\infty dk'\ \frac{k'}{k'^2-k^2}\tilde{F}(k'). \tag{15}$$

The expression for the dipole–dipole interaction tensor, $\tilde{V}(k)$, was derived in Appendix A, $d\Omega=\sin\theta d\theta d\phi$. Since the two tensors, $\tilde{F}(k)$ and $\tilde{V}(k)$, are related to each other by the Kramers–Kronig relationship, one can in principle calculate $\tilde{V}(k)$ by obtaining $\tilde{F}(k)$ and vice versa. As can be seen in the definition of $\tilde{F}(k)$ in Eq. (15), $\tilde{F}(k)$ contains information on the spatial correlation of displacement field operator $\langle\hat{D}_{k\lambda}(\mathbf{R}_A)\hat{D}_{k\lambda}(\mathbf{R}_B)\rangle_{\text{vac}}$. Equation (14) involves both the elastic scattering of the fluctuating vacuum field by molecules and the inelastic virtual processes, such as the absorption and emission of the virtual photons. As a matter of fact, the two tensors, $\tilde{F}(k)$ and $\tilde{V}(k)$, are proportional to the imaginary and real parts of the Green function of the fluctuating vacuum electric field,[33,34] where the Green function is defined by the Fourier component of the antisymme-

trized time correlation function of the electric field operator. A detailed derivation of $\widetilde{F}(k)$ by using Eq. (15) with proper mode functions of the quantized electromagnetic fields is given in Appendix C. Then $\widetilde{V}(k)$ can be calculated from Eq. (15).

In order to rewrite the van der Waals interaction energy in Eq. (14), we define

$$\widetilde{G}(k) \equiv \widetilde{V}(k) + i\widetilde{F}(k), \tag{16}$$

to obtain

$$\Delta E = -\frac{\hbar c}{2\pi} \operatorname{Im} \int_0^\infty dk \ \operatorname{Tr}[\widetilde{\alpha}_{\mathrm{A}}(\omega_k)\widetilde{G}(k)\widetilde{\alpha}_{\mathrm{B}}(\omega_k)\widetilde{G}^+(k)]. \tag{17}$$

We find that it is useful to rewrite Eq. (17), which is given by an integral over the real frequency, as an integral over the imaginary frequency $k \to i\kappa$ with $\kappa > 0$ so that we have

$$\Delta E = \frac{\hbar c}{2\pi} \int_0^\infty d\kappa \ \operatorname{Tr}[\widetilde{\alpha}_{\mathrm{A}}(i\kappa c)\widetilde{\mathbf{G}}(i\kappa)\widetilde{\alpha}_{\mathrm{B}}(i\kappa c)\widetilde{\mathbf{G}}^+(i\kappa)]. \tag{18}$$

Here $\widetilde{\mathbf{G}}(i\kappa)$ is proportional to the temperature Green's function, which is defined in terms of the Matsubara electromagnetic field operators.[33] As well-known, the temperature Green's function is related to the retarded Green function by using the analytic continuation procedure rotating the real frequency axis into the pure imaginary axis. We wish to emphasize that, even though we used a set of fully quantized electromagnetic fields, the van der Waals interaction potential reduces to a problem of calculating the spatial correlation function of the fields. Moreover those mode functions are determined by the *classical* Helmholtz equation with the proper boundary conditions.

A. Anisotropic molecular polarizability

Instead of considering an arbitrary polarizability, we shall focus on the symmetric top molecules. The polarizability tensor for a symmetric top molecule can be expressed most generally as

$$\widetilde{\alpha}(\omega) = \alpha(\omega)\widetilde{I} - \beta(\omega)(\widetilde{I} - 3\hat{u}\hat{u}), \tag{19}$$

where $\hat{u}$ denotes the unit vector which lies along the principle axis of the symmetric top molecule. By designating $\alpha_{\parallel}(\omega)$ and $\alpha_{\perp}(\omega)$ as the polarizabilities of the molecule along the symmetry axis and along any axis perpendicular to $\hat{u}$, respectively, we defined the isotropic and anisotropic parts of the molecular polarizability as

$$\begin{aligned} \alpha(\omega) &= \frac{1}{3}\{\alpha_{\parallel}(\omega) + 2\alpha_{\perp}(\omega)\}, \\ \beta(\omega) &= \frac{1}{3}\{\alpha_{\parallel}(\omega) - \alpha_{\perp}(\omega)\}. \end{aligned} \tag{20}$$

It should be noted that the polarizability tensor given in Eq. (19) is symmetric and that the anisotropic part, proportional to $\beta(\omega)$, is traceless.

B. van der Waals interaction in short distance limit

Using the proper mode functions of fully quantized electromagnetic field near two planar surfaces, we calculated $\widetilde{F}(k)$ in Appendix C. In the short distance limit, as discussed in Appendix C, the Fresnel reflection and transmission coefficients are assumed to be independent on the incidence angle θ and the contributions from multiple (more than once) reflections by the two surfaces are ignored. Moreover, the retardation effects caused by the finite speed of light can be ignored. In this limit, the Green function, $\widetilde{\mathbf{G}}(i\kappa)$, in the imaginary frequency domain can be approximately given as

$$\begin{aligned} \widetilde{\mathbf{G}}(i\kappa) &= \widetilde{\mathbf{G}}_{\mathrm{I}}^{\mathrm{even}}(i\kappa) + \widetilde{\mathbf{G}}_{\mathrm{I}}^{\mathrm{odd}}(i\kappa) + \widetilde{\mathbf{G}}_{\mathrm{II}}^{\mathrm{even}}(i\kappa) + \widetilde{\mathbf{G}}_{\mathrm{II}}^{\mathrm{odd}}(i\kappa) \\ &\cong C_0(i\kappa)\,\frac{\widetilde{I} - 3\hat{r}\hat{r}}{r^3} + C_{\mathrm{I}}(i\kappa)\,\frac{\widetilde{I}' - 3\hat{R}_{\mathrm{I}}\hat{R}_{\mathrm{I}}'}{R_{\mathrm{I}}^3} \\ &\quad + C_{\mathrm{II}}(i\kappa)\,\frac{\widetilde{I}' - 3\hat{R}_{\mathrm{II}}\hat{R}_{\mathrm{II}}'}{R_{\mathrm{II}}^3}, \end{aligned} \tag{21}$$

where the coefficients in the imaginary frequency domain are

$$\begin{aligned} C_0(i\kappa) &\equiv \frac{1}{2}\left(\left[\frac{2\sqrt{\epsilon_1(i\kappa)}}{\epsilon_1(i\kappa)+1}\right]^2\left\{1 + \left[\frac{\epsilon_3(i\kappa)-1}{\epsilon_3(i\kappa)+1}\right]^2\right\}\right. \\ &\quad \left. + \left[\frac{2\sqrt{\epsilon_3(i\kappa)}}{\epsilon_3(i\kappa)+1}\right]^2\left\{1 + \left[\frac{\epsilon_1(i\kappa)-1}{\epsilon_1(i\kappa)+1}\right]^2\right\}\right), \\ C_{\mathrm{I}}(i\kappa) &\equiv -\left[\frac{2\sqrt{\epsilon_1(i\kappa)}}{\epsilon_1(i\kappa)+1}\right]^2\left[\frac{\epsilon_3(i\kappa)-1}{\epsilon_3(i\kappa)+1}\right], \\ C_{\mathrm{II}}(i\kappa) &\equiv -\left[\frac{2\sqrt{\epsilon_3(i\kappa)}}{\epsilon_3(i\kappa)+1}\right]^2\left[\frac{\epsilon_1(i\kappa)-1}{\epsilon_1(i\kappa)+1}\right]. \end{aligned} \tag{22}$$

In Eq. (21), $\hat{r}$, $\hat{R}_{\mathrm{I}}$, and $\hat{R}_{\mathrm{II}}$ are the unit vectors of $\mathbf{r}$, $\mathbf{R}_{\mathrm{I}}$, and $\mathbf{R}_{\mathrm{II}}$, respectively. I' and R' are defined in Eq. (C4). It should be noted that the dielectric functions in the above equations are evaluated in the imaginary frequency so that they are monotonously decreasing function with respect to the imaginary frequency. The first term in Eq. (21) represents the contributions from direct interaction without involving any reflection of a virtual photon by the surfaces, whereas the second and third terms correspond to those involving a single reflection by the lower surface and that by the upper surface, respectively. Inserting the two polarizability tensors defined in Eq. (19) and the Green functions in Eq. (21) into Eq. (18) gives the van der Waals interaction,

$$\begin{aligned} \Delta E = -\frac{\hbar c}{2\pi}\int_0^\infty d\kappa \left\{ \frac{C_0^2\Lambda_{0,0}}{r^6} + \frac{C_0 C_{\mathrm{I}}\Lambda_{0,\mathrm{I}}}{r^3 R_{\mathrm{I}}^3} + \frac{C_0 C_{\mathrm{II}}\Lambda_{0,\mathrm{II}}}{r^3 R_{\mathrm{II}}^3} \right. \\ \left. + \frac{C_{\mathrm{I}}^2\Lambda_{\mathrm{I,I}}}{R_{\mathrm{I}}^6} + \frac{C_{\mathrm{II}}^2\Lambda_{\mathrm{II,II}}}{R_{\mathrm{II}}^6} + \frac{C_{\mathrm{I}}C_{\mathrm{II}}\Lambda_{\mathrm{I,II}}}{R_{\mathrm{I}}^3 R_{\mathrm{II}}^3} \right\}, \end{aligned} \tag{23}$$

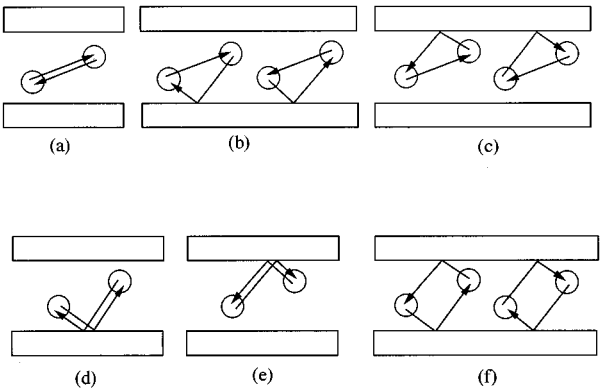

FIG. 2. Six different contributions to the van der Waals interaction are shown [see Eq. (23) and discussion below Eq. (25)]. Exchange of two virtual photons are represented by arrows. (a)–(f) correspond to the first to the sixth terms in Eq. (23), respectively.

where, for m, $n=0$,I,II,

$$\begin{aligned}\Lambda_{m,m}(i\kappa)=&\,\mathrm{Tr}\{\alpha_{\mathrm{A}}\alpha_{\mathrm{B}}\tilde{T}_m\tilde{T}_m^+-\alpha_{\mathrm{A}}\beta_{\mathrm{B}}\tilde{T}_m\tilde{\tau}_{\mathrm{B}}\tilde{T}_m^+\\&-\beta_{\mathrm{A}}\alpha_{\mathrm{B}}\tilde{\tau}_{\mathrm{A}}\tilde{T}_m\tilde{T}_m^++\beta_{\mathrm{A}}\beta_{\mathrm{B}}\tilde{\tau}_{\mathrm{A}}\tilde{T}_m\tilde{\tau}_{\mathrm{B}}\tilde{T}_m^+\}\\\Lambda_{m,n}(i\kappa)=&\,\mathrm{Tr}\{\alpha_{\mathrm{A}}\alpha_{\mathrm{B}}(\tilde{T}_m\tilde{T}_n^++\tilde{T}_n\tilde{T}_m^+)-\alpha_{\mathrm{A}}\beta_{\mathrm{B}}(\tilde{T}_m\tilde{\tau}_{\mathrm{B}}\tilde{T}_n^+\\&+\tilde{T}_n\tilde{\tau}_{\mathrm{B}}\tilde{T}_m^+-\beta_{\mathrm{A}}\alpha_{\mathrm{B}}(\tilde{\tau}_{\mathrm{A}}\tilde{T}_m\tilde{T}_n^++\tilde{\tau}_{\mathrm{A}}\tilde{T}_n\tilde{T}_m^+)\\&+\beta_{\mathrm{A}}\beta_{\mathrm{B}}(\tilde{\tau}_{\mathrm{A}}\tilde{T}_m\tilde{\tau}_{\mathrm{B}}\tilde{T}_n^++\tilde{\tau}_{\mathrm{A}}\tilde{T}_n\tilde{\tau}_{\mathrm{B}}\tilde{T}_m^+)\end{aligned}\tag{24}$$

with

$$\begin{aligned}&\tilde{\tau}_{\mathrm{A}}-3\hat{u}_{\mathrm{A}}\hat{u}_{\mathrm{A}},\\&\tilde{\tau}_{\mathrm{B}}=\tilde{I}-3\hat{u}_{\mathrm{B}}\hat{u}_{\mathrm{B}},\\&\tilde{T}_0=\tilde{T}-3\hat{r}\hat{r},\\&\tilde{T}_{\mathrm{I}}=\tilde{I}'-3\hat{R}_{\mathrm{I}}\hat{R}_{\mathrm{I}}',\\&\tilde{T}_{\mathrm{II}}=\tilde{I}'-3\hat{R}_{\mathrm{II}}\hat{R}_{\mathrm{II}}'.\end{aligned}\tag{25}$$

Equations (23) with (24) and (25) are the main results in this section, and show complex dependence on the distances between real molecules as well as between real and image molecules. Only the first term is inversely proportional to the sixth power of the direct intermolecular distance. Therefore, the first term is the largest one since both R_{I} and R_{II} are always larger than the direct distance through the free space. The physical meaning of each term can be understood by considering the exchange process of a couple of virtual photons. As shown in Fig. 2(a), the first term on the right-hand side of Eq. (23) corresponds to the case when the two virtual photons are exchanged via free space. On the other hand, the second and third terms [Figs. 2(b) and 2(c), respectively] involve a single reflection by the lower and upper surfaces, respectively. The fourth and fifth terms [Figs. 2(d) and 2(e)] involve two reflections by the same surface, whereas the sixth term [Fig. 2(f)] does two reflections—once by each surface.

The general expression given in Eq. (23) is very complicated because of the geometrical factors, though it is quite straightforward to rewrite them in terms of angles and distances defined in Fig. 1(b). Instead of discussing Eq. (23) more in detail, we shall consider several limiting cases that should be found useful in practical calculations. Since the van der Waals interaction between either isotropic or anisotropic molecules in vacuum has been studied extensively, we shall not consider those cases in the following sections.

IV. SINGLE DIELECTRIC SURFACE

We shall consider, in this section, the case when the two molecules are in the vicinity of a single dielectric surface. Let us assume that the upper dielectric medium is replaced with an infinite vacuum. In this case, the dielectric function $\epsilon_1(i\kappa)$ equals to 1, that is the transmission coefficient t_{12} becomes unity whereas $r_{21}=0$. Then the third, fifth, and sixth terms on the right-hand side of Eq. (23) vanish.

A. Isotropic molecules

If the two molecular polarizabilities are isotropic, from Eq. (23) we find

$$\begin{aligned}\Delta E=&-\frac{3\hbar}{\pi r^6}I_0^{\alpha\alpha}+\frac{\hbar(2-3\cos 2\psi-3\cos 2\chi)}{2\pi r^3R_{\mathrm{I}}^3}I_1^{\alpha\alpha}\\&-\frac{3\hbar}{\pi R_{\mathrm{I}}^6}I_2^{\alpha\alpha},\end{aligned}\tag{26}$$

where

$$\begin{aligned}I_0^{\alpha\alpha}&=\int_0^\infty d\kappa\,\alpha_{\mathrm{A}}(i\kappa)\alpha_{\mathrm{B}}(i\kappa),\\I_1^{\alpha\alpha}&=\int_0^\infty d\kappa\left[\frac{\epsilon_3(i\kappa)-1}{\epsilon_3(i\kappa)+1}\right]\alpha_{\mathrm{A}}(i\kappa)\alpha_{\mathrm{B}}(i\kappa),\\I_2^{\alpha\alpha}&=\int_0^\infty d\kappa\left[\frac{\epsilon_3(i\kappa)-1}{\epsilon_3(i\kappa)+1}\right]^2\alpha_{\mathrm{A}}(i\kappa)\alpha_{\mathrm{B}}(i\kappa).\end{aligned}\tag{27}$$

Equations (26) with (27) are exactly identical to MacLachlan's results[8,34,37] {note that the angles defining the geometry [see Fig. 1(b)] are defined differently from MacLachlan's[8]}. In the definitions of three integrals, the superscript, "$\alpha\alpha$," denotes that the integrals involve the isotropic polarizabilities in the integrand. The first term is just the van der Waals interaction in the free space—London's result can be obtained by assuming that the molecular polarizability is determined by a single frequency, so that the integration over the imaginary frequency can be performed by using residue theorem. The second term represents the vdW interaction when one of the two virtual photons is reflected by the surface. Because of the interference effect between the direct dipolar field and the reflected dipolar field, the magnitude of the second term becomes strongly dependent on the detailed geometry. For example when the two molecules are located parallel to the surface and separated far apart, the second term becomes positive so that the overall vdW interaction decreases compared to that in the free space. The third term corresponds to the contribution from the interaction between the induced dipole in the free space

and the induced *image* dipole created in the dielectric medium. They are separated by the distance R_I. Usually the third term is much smaller than the second one, except when the two molecules are far apart as well as when they both are close to the surface.

These results has been used in understanding lateral interactions between adatoms,[35–37] where the two-dimensional flat film is normally assumed. For example, Rauber *et al.*[38] showed that the reduction in the potential well depth of 15%–20% from the free space values for the inert gas atoms near graphite surface can be assigned to the additional (second) term in Eq. (26).

In order to obtain simpler results with retaining salient features of a dielectric (metal) surface, we further use a free-electron-like (Thomas–Fermi model) dielectric function[39,40]

$$\epsilon(i\kappa)=1+\frac{\omega_p^2}{\kappa^2}, \tag{28}$$

where ω_p is the plasma frequency, which is the characteristic resonance frequency of absorption of the electrons in the metal. For the sake of simplicity, if the two molecules are identical and the molecular polarizability is determined by a single transition frequency, ω_0, i.e.,

$$\alpha(i\kappa)=2|\mu|^2\frac{\omega_0}{\hbar(\omega_0^2+\kappa^2)}, \tag{29}$$

the three integrals defined in Eq. (37) can be calculated, within these approximations to the dielectric function and the molecular polarizabilities,

$$I_0^{\alpha\alpha}=\frac{\pi\omega_0\alpha^2(0)}{4},$$
$$I_1^{\alpha\alpha}=\frac{\pi\omega_0\alpha^2(0)}{4}\left[\frac{\gamma^2+2\gamma}{(\gamma+1)^2}\right], \tag{30}$$
$$I_2^{\alpha\alpha}=\frac{\pi\omega_0\alpha^2(0)}{4}\left[\frac{\gamma(\gamma^2+3\gamma+1)}{(\gamma+1)^3}\right].$$

Here γ is the ratio of the surface-plasmon frequency to the molecular transition frequency,

$$\gamma=\frac{\omega_p/\sqrt{2}}{\omega_0}. \tag{31}$$

If the ratio γ becomes large, that is, the surface acts like a good mirror, all three integrals given in Eqs. (30) become identical. In this limit, the surface boundary effects will be maximized. On the other hand, as the ratio γ approaches zero, the last two integrals, $I_1^{\alpha\alpha}$ and $I_2^{\alpha\alpha}$, decreases to zero, so that the boundary effects become negligible, as expected.

In the limiting case both when the two molecules are far apart and located side by side (''lateral'') on the dielectric surface ($\psi=\chi\cong\pi/2$ and $r\cong R_I$) and when the ratio γ approaches a large number, the total vdW interaction energy reduces to approximately two-thirds of that in the free space. This is demonstrated by a numerical evaluation of Eq. (26) with Eq. (30) in Fig. 3(a), where the ratio of the vdW interaction between two isotropic molecules near a surface to that in the free space is calculated. Here the dielectric surface is fully characterized by the ratio γ that is assumed to be 2. *The distance between the molecule A and the surface is assumed to be unity*, and the distance between molecules is scaled by this unit distance in the following calculations. As the two molecules approaches to each other the surface boundary effect decreases since the additional terms [the second and third terms in Eq. (26)] are negligibly small in this limit. If one of the two molecules is on top of the other (''vertical''), the intermolecular interaction becomes larger than that in the free space as shown in Fig. 3(a).

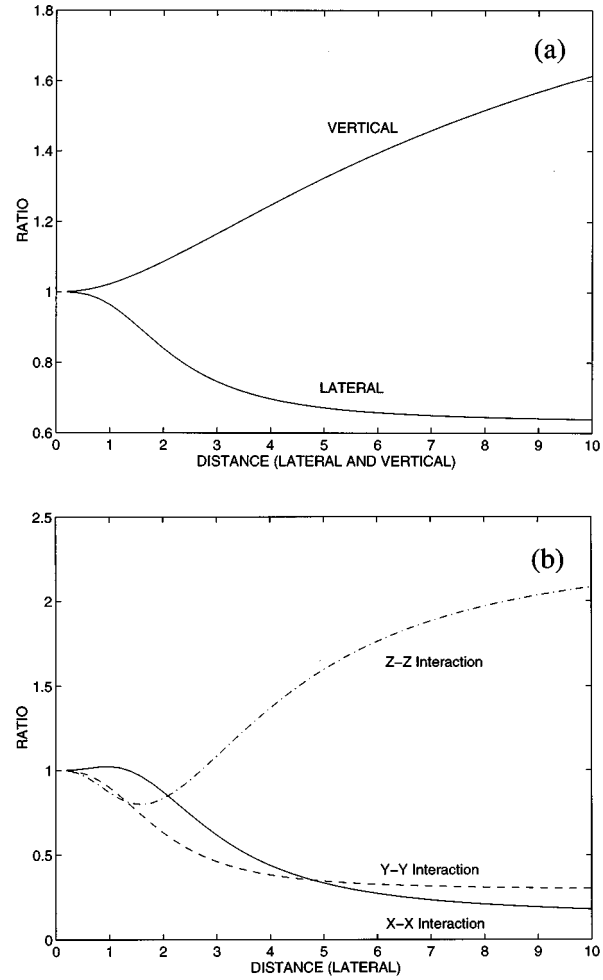

FIG. 3. The ratios of the van der Waals interaction between two isotropic molecules (a) or two anisotropic molecules (b) near a *single* dielectric surface to that in the *free* space are plotted. The ratio of the surface-plasmon frequency to the optical transition frequency, γ, is assumed to be 2 [see Eq. (31)]. $\alpha_\parallel(\omega)/\alpha_\perp(\omega)=3$. The distance between the molecule A and the surface is assumed to be unity, and the distance between molecules is scaled by this unit distance.

B. Anisotropic molecules

In case when the two molecules near a surface are anisotropic, one needs to consider the complicated geometrical factors given in Eqs. (23). Since it is very tedious to rewrite the geometrical factors in terms of angles of the two molecules with respect to the surfaces, we instead present nu-

merical calculations to survey the general trends. To this end, we assume that the surface and molecular polarizabilities are given by the forms in Eqs. (28) and (29), respectively, except that the ratio of the parallel polarizability $\alpha_{\parallel}(\omega)$ to the perpendicular component $\alpha_{\perp}(\omega)$ is assumed to be 3. The ratio γ defined in Eq. (31) equals 2.

In Fig. 3(b), the ratios of the vdW interactions near a surface to those in the free space are shown, where we consider three different cases when the molecular principal axes lie along three different axes in the laboratory coordinate space. Again it should be noted that the two molecules are in the $y-z$ plane (see Fig. 1). When the two molecular axes are parallel to either the x- or y-axis, the vdW interaction decreases compared to that in the free space. In contrast, the $z-z$ interaction is enhanced by the existence of the surface. This can be understood by using the image picture. Suppose the two molecular axes lie along the z-axis—that is, the principal axes are perpendicular to the surface plane. Then the instantaneous induced dipole at the center of a molecule is more likely to be aligned to be perpendicular to the surface plane, because the parallel component of the polarizability is larger than the perpendicular one. The image dipole thus induced in the dielectric medium is oriented with the same direction with the induced dipole of the molecule A. Therefore, the magnitude of the combined dipole moment is larger than that in the free space, which will be shown up as an increased vdW interaction energy when the two molecules are well separated. However when they are in close proximity, the overall interaction is not monotonic as can be seen in Fig. 3(b). Similar discussions with the image picture are applicable to the other two cases, $x-x$ and $y-y$ interactions, though in these cases the cancellation between the induced dipole of a real molecule and the induced *image* dipole will make the overall vdW interactions decrease in comparison to those in the free space.

In comparison to the vdW interaction between two *isotropic* molecules, one of the most distinctive features in the interaction between *anisotropic* molecules is that the alignment of the two molecules is very important factor in determining the role of the dielectric surface. Depending on the molecular alignments, the surface enhances or suppresses the vdW interaction in the vicinity of a dielectric surface—note that a similar observation was also made in studies on the spontaneous emission rate near a dielectric surface.[1–3]

V. TWO DIELECTRIC SURFACES

When the two molecules are located in between two surfaces, one can expect that the boundary effects induced by a single surface discussed above would perhaps be enhanced. Indeed as we show in Figs. 4(a) and 4(b), there are strong modifications of the vdW interaction strength. For example, when two isotropic molecules are located exactly in between the two surfaces with their intermolecular axis parallel to the surfaces (lying along the x-axis), the ratio of the vdW interaction to that in the free space is shown in Fig. 4(a). Here we assume that the two dielectric media are identical. The trend observed in Fig. 4(a) is identical to the case when two isotropic molecules are near a single surface [see Fig. 3(a) ''lateral'']. Similarly, we calculated the vdW interaction between two anisotropic molecules in a planar cavity in Fig. 4(b). Since we assumed that the geometry is symmetric—the two dielectrics are identical and distances between each surface and the two molecules are also identical, the quantitative trends of enhancement or suppression are found to be identical to Fig. 3(b).

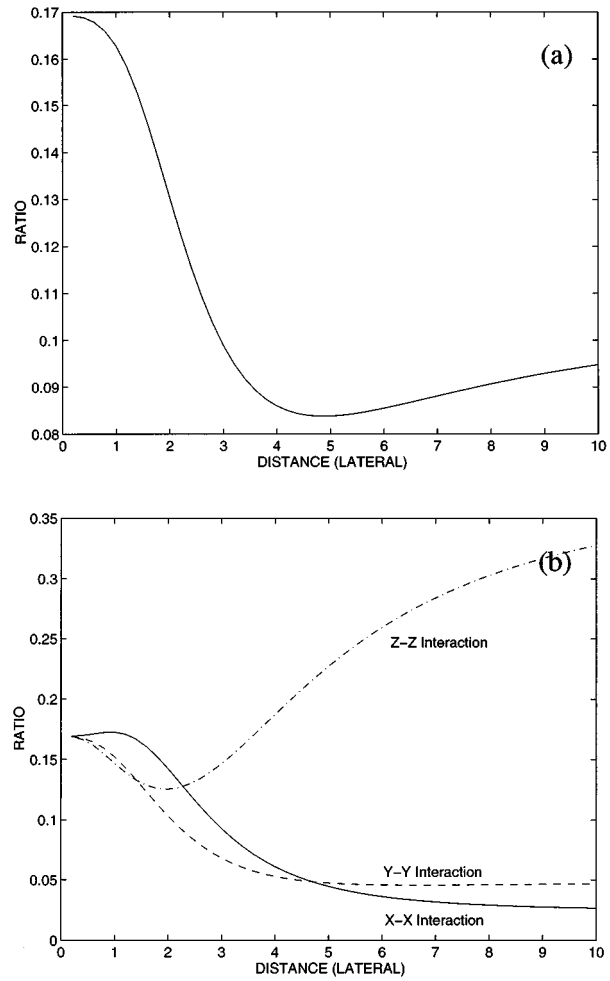

FIG. 4. The ratios of the van der Waals interaction between two isotropic molecules (a) or two anisotropic molecules (b) in between *two dielectric surfaces* to that in the *free* space are plotted. The ratio of the surface-plasmon frequency to the optical transition frequency, γ, is assumed to be 2. $\alpha_{\parallel}(\omega)/\alpha_{\perp}(\omega)=3$. The two molecules are located exactly in between the two surfaces so that the lateral intermolecular interaction is only considered in this figure.

Although the boundary effect induced by two surfaces is qualitatively identical to that by a single surface, the overall magnitude of the vdW interaction energy in a planar cavity is suppressed in comparison to those in vacuum or in the presence of a single dielectric surface, and also strongly depends on the dielectric properties of the two media. In order to show this tendency, we numerically calculate Eq. (23) when the intermolecular distance between two isotropic molecules is much smaller than the distances between molecules and surfaces—this is the short-intermolecular-distance limit in

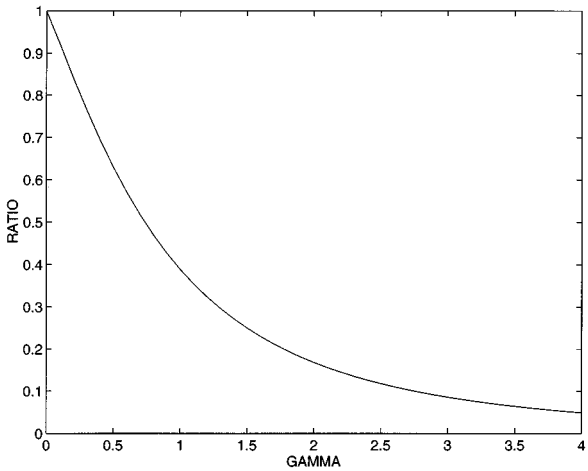

FIG. 5. The ratio of the van der Waals interaction energy between two isotropic molecules in between two dielectric surfaces to that in the free space is plotted as a function of γ in the short-intermolecular-distance limit. The two dielectrics are identical. The dielectric functions and polarizabilities are assumed to be described by Eqs. (28) and (29), respectively.

Fig. 4(a). Here the Thomas–Fermi model [see Eq. (28)] and Eq. (29) are used for the dielectric functions and polarizabilities, respectively. The two dielectrics are identical. In this limit, the first term in Eq. (23) dominates. The ratio of the vdW interaction energy in between two surfaces to that in the vacuum space as a function of $\gamma(=\omega_p/\sqrt{2}\omega_0)$ is plotted in Fig. 5. As the transmissivity decreases, that is, γ increases, the vdW interaction in between two dielectrics decreases. For instance, the vdW interaction energy of two isotropic molecules is about one-fifth of that in the free space, when we assume that the ratio (γ) of the surface-plasmon frequency to that of the molecular transition frequency [see Eq. (31)] equals to 2. This behavior can be understood as following. When there is a *single* surface, the amplitude of the field mode around the surface is identical to that in the free space, though the mean square fluctuation amplitude of the electromagnetic field in the vicinity of the surface dramatically differs from that in the free space. In order to illustrate this point, let us consider the temperature Green functions, Eqs. (21) and (22), in the cases of both the free space $[\epsilon_1(i\kappa)=\epsilon_3(i\kappa)=1]$ and the single dielectric surface $[\epsilon_1(i\kappa)=1$ and $\epsilon_3(i\kappa)>1]$, which are, respectively,

$$\tilde{\mathbf{G}}^0(i\kappa)=\frac{\tilde{I}-3\hat{r}\hat{r}}{r^3}$$

and

$$\tilde{\mathbf{G}}^{s.s.}(i\kappa)=\frac{\tilde{I}-3\hat{r}\hat{r}}{r^3}-\left[\frac{\epsilon_3(i\kappa)-1}{\epsilon_3(i\kappa)+1}\right]\frac{\tilde{I}'-3\hat{R}_{\mathrm{I}}\hat{R}'_{\mathrm{I}}}{R_{\mathrm{I}}^3}.$$

In both cases, the leading term is the usual dipole–dipole interaction tensor in the free space. However, in the case when the vacuum space is confined by two dielectric media, the intensity of the mode in the vacuum region becomes proportional to the square of the transmission coefficients, which appears in Eqs. (22) as

$$t_{12}^2=\left[\frac{2\sqrt{\epsilon_1(i\kappa)}}{\epsilon_1(i\kappa)+1}\right]^2 \quad \text{and} \quad t_{32}^2=\left[\frac{2\sqrt{\epsilon_3(i\kappa)}}{\epsilon_3(i\kappa)+1}\right]^2,$$

which are always less than or equal to unity. Thus, *in the short distance limit, the magnitude of the van der Waals interaction can be suppressed by the two dielectric surfaces with a large dielectric function*. Here we should emphasize again that, because Eq. (21) was obtained in the short-distance limit, contributions from multiple reflections were ignored. If the reflectivity of the two dielectric media becomes close to one (that is the transmissivity from the dielectric to the free space region is equal to zero), one has to take into account the multiple reflection effects. In particular, these effects will be important when the two molecules are far apart and the distances between molecules and surfaces are comparatively small.

VI. SUMMARY

Using the mode functions of the quantized electromagnetic field, the Green function, in the imaginary frequency, in a planar cavity was calculated in the short-distance limit. The van der Waals interaction between two isotropic or anisotropic molecules are calculated by considering the dipole–dipole interaction between two vacuum-field-induced dipoles. When a pair of molecules are in the vicinity of surfaces, the interference effects between the dipolar field and the reflected dipolar field are found to be important. In particular, when the two molecules are anisotropic, the surface can enhance or suppress the van der Waals interaction depending on the molecular alignments. A simple image picture was used to describe these effects. It was shown that, in case of two planar surfaces, the general trends are found to be identical to the case of a single surface. However, since the mode intensity between two dielectric media is decreased relative to that near a single surface, the absolute magnitude of the van der Waals interaction in a planar cavity is smaller than those in the free space or near a single surface. Consequently, the estimate of the van der Waals interaction between atoms or molecules in the confined geometry by using the parameters obtained from the gas-phase experiment is likely to be strongly deviated from the actual value in this circumstance.

ACKNOWLEDGMENT

Financial support by the National Science Foundation is gratefully acknowledged.

APPENDIX A: CALCULATION OF THE DIPOLE–DIPOLE INTERACTION TENSOR

In this appendix we derive an expression for the general dipole–dipole interaction tensor, which is valid for any arbitrary boundary conditions. McLone and Power[32] considered the resonance interaction of a pair of dipoles including the retardation effect in the *free* space. We generalize their result for arbitrary planar boundary conditions imposed by the macroscopic dielectric surfaces. In order to obtain the dipole–dipole potential tensor we need to use second-order

perturbation theory with respect to the original interaction Hamiltonian, $H_{\mathrm{I}}=-\hat{\mu}_{\mathrm{A}}\cdot D(\mathbf{R}_{\mathrm{A}})-\hat{\mu}_{\mathrm{B}}\cdot D(\mathbf{R}_{\mathrm{B}})$. From the second-order perturbation theory, the dipole coupling interaction is

$$M=\sum_{\mathrm{I}} \frac{\langle f|H_{\mathrm{I}}|I\rangle\langle I|H_{\mathrm{I}}|i\rangle}{E_{\mathrm{I}}-E_m}, \tag{A1}$$

where the initial and final states are product states given by

$$\begin{aligned}|i\rangle&=|e^{\mathrm{A}},g^{\mathrm{B}};\{0\}\rangle,\\ |f\rangle&=|g^{\mathrm{A}},e^{\mathrm{B}};\{0\}\rangle.\end{aligned} \tag{A2}$$

Here, for example, g^{A} and e^{B} denote the ground state of the A molecule and the excited state of the B molecule, respectively. $\{0\}$ denotes the vacuum state of the field. For initial and final states given above, there are two possible intermediate states,

$$|I\rangle=|e^{\mathrm{A}},e^{\mathrm{B}};1_k\rangle \quad\text{and}\quad |I\rangle=|g^{\mathrm{A}},g^{\mathrm{B}};1_k\rangle. \tag{A3}$$

The former intermediate state involves two excited states of both A and B molecules and one excitation of the **k**th field. The latter one involves two ground states of A and B molecules and one excitation of the **k**th field. Although we considered vacuum states for the both initial and final field states, we found that the dipole coupling interaction M defined in Eq. (A1) does not depend on the initial photon numbers as long as the final field state is identical to that of the initial state.

Inserting the electric displacement field operator given in Eq. (8) and electric dipole operators in Eq. (7), we find the dipole coupling interaction is

$$M=\overline{\mu_{\mathrm{A}}}\cdot\widetilde{V}(k_p)\cdot\overline{\mu_{\mathrm{B}}}, \tag{A4}$$

where $\overline{\mu}$ is the electric dipole matrix element, and the general dipole–dipole interaction tensor can be defined as

$$\widetilde{V}(k_p=\omega_p/c)\equiv\sum_{k\lambda}\frac{2\pi\hbar\omega_k}{V}\left[\frac{\mathbf{f}_{k\lambda}(\mathbf{R}_{\mathrm{A}})\mathbf{f}^*_{k\lambda}(\mathbf{R}_{\mathrm{B}})}{-\hbar\omega_p-\hbar\omega_k}+\frac{\mathbf{f}^*_{k\lambda}(\mathbf{R}_{\mathrm{A}})\mathbf{f}_{k\lambda}(\mathbf{R}_{\mathrm{B}})}{\hbar\omega_p-\hbar\omega_k}\right]. \tag{A5}$$

This expression is valid regardless of the macroscopic boundary conditions. Here ω_p is the transition frequency of the dipole assuming that the transition frequencies of the two dipoles are identical. In case when the two molecules are in the free space, the mode functions are given by $\exp(i\mathbf{kr})$. Then after summing over $(\mathbf{k},\lambda)$, we can recover the result obtained by McLone and Power.[32]

The dipole–dipole potential tensor in Eq. (A5) is determined by the spatial correlation, such as $\mathbf{f}_{k\lambda}(\mathbf{R}_{\mathrm{A}})\mathbf{f}^*_{k\lambda}(\mathbf{R}_{\mathrm{B}})$. We separate the real and imaginary parts of $\mathbf{f}_{k\lambda}(\mathbf{R}_{\mathrm{A}})\mathbf{f}^*_{k\lambda}(\mathbf{R}_{\mathrm{B}})$ and use the fact that the term containing imaginary part of $\mathbf{f}_{k\lambda}(\mathbf{R}_{\mathrm{A}})\mathbf{f}^*_{k\lambda}(\mathbf{R}_{\mathrm{B}})$ vanishes when the summation over $(\mathbf{k},\lambda)$ is performed. Finally the dipole–dipole potential tensor becomes

$$\widetilde{V}(k_p)\equiv\frac{4\pi}{V}\,\mathrm{Re}\sum_{k\lambda}\frac{k^2}{k_p^2-k^2}\,\mathbf{f}_{k\lambda}(\mathbf{R}_{\mathrm{A}})\mathbf{f}^*_{k\lambda}(\mathbf{R}_{\mathrm{B}}). \tag{A6}$$

This is Eq. (15) used in Sec. III. The authors presented the theoretical derivation of the dipole–dipole interaction tensor in the presence of a single dielectric surface in Ref. 41.

APPENDIX B: SPATIAL MODE FUNCTIONS IN PLANAR MICROCAVITY

In this appendix, we summarize the well-known mode functions of the quantized electromagnetic field in a planar microcavity (Fabry–Perot cavity).[6,42] The geometrical details of the interfaces and spatial coordinates were given in Fig. 1, where the origin of the z-axis is taken at the boundary between the upper dielectric medium and the intermediate free space. The x and y axes lie within the upper interfaces. We choose the coordinate system to make the two molecules lie within the $x-z$ plane [see Fig. 1(b)]. There are two classes of modes, one is originated from the transmitted incident field propagating downward and the other from that propagating upward. Each triplet consists of the incident, reflected, and transmitted modes in the free space between the two dielectric media. Here the reflected and transmitted fields could be created by multiple reflections inside of the cavity. Instead of presenting detailed expressions of the various modes, in this appendix we summarize the type I mode functions, which will be used in the next appendix to calculate spatial correlation function of the electric field. For detailed discussions on the quantization of Fresnel modes as well as a complete list of the mode functions near two planar surfaces, the readers may refer to Khosravi and Loudon[6] and De Martini *et al.*[42]

The type I Fresnel mode functions associated with the initially downward incident field in the free space can be recast in the form

$$\mathbf{f}^I_{k\lambda}(\mathbf{R})=\hat{e}^i_{k\lambda}\,\exp(i\mathbf{k}_+\cdot\mathbf{R})+\hat{e}^r_{k\lambda}\,\exp(i\mathbf{k}_-\cdot\mathbf{R}), \tag{B1}$$

where $\mathbf{k}_+$ and $\mathbf{k}_-$ are the wave vectors of the incident and reflected modes, that are propagating downward and upward, respectively,

$$\begin{aligned}\mathbf{k}_+&=k(\sin\theta\cos\phi,\sin\theta\sin\phi,\cos\theta),\\ \mathbf{k}_-&=k(\sin\theta\cos\phi,\sin\theta\sin\phi,-\cos\theta).\end{aligned} \tag{B2}$$

Here $k=\omega_k/c$. The transverse field includes two orthogonal components that are normal $(\lambda=\perp)$ and parallel $(\lambda=\parallel)$ to the incident plane. Then the unit vectors of the incident and reflected modes are

$$\begin{aligned}\hat{e}^i_{\mathbf{k}\perp}&=\frac{t^{\perp}_{12}}{\Delta_{\perp}}(\sin\phi,-\cos\phi,0),\\ \hat{e}^i_{\mathbf{k}\parallel}&=\frac{t^{\parallel}_{12}}{\Delta_{\parallel}}(\cos\theta\cos\phi,\cos\theta\sin\phi,-\sin\theta),\\ \hat{e}^r_{\mathbf{k}\perp}&=\frac{t^{\perp}_{12}r^{\perp}_{23}}{\Delta_{\perp}}(\sin\phi,-\cos\phi,0),\\ \hat{e}^r_{\mathbf{k}\parallel}&=-\frac{t^{\parallel}_{12}r^{\parallel}_{23}}{\Delta_{\parallel}}(\cos\theta\cos\phi,\cos\theta\sin\phi,\sin\theta),\end{aligned} \tag{B3}$$

where

$$\Delta_\lambda \equiv 1 - r_{21}^\lambda r_{23}^\lambda \exp(2ikd\cos\theta). \tag{B4}$$

By defining the Lifshitz variables as

$$\begin{aligned} p &= \cos\theta, \\ s_1 &= \sqrt{\epsilon_1(\omega) - 1 + p^2}, \\ s_3 &= \sqrt{\epsilon_3(\omega) - 1 + p^2}, \end{aligned} \tag{B5}$$

the Fresnel reflection and transmission coefficients for the normal and parallel transverse modes are written as,[43]

(i) reflection coefficients for $n=1$ or 3,

$$\begin{aligned} r_{2n}^\perp &= -r_{n2}^\perp = \frac{p - s_n}{p + s_n}, \\ r_{2n}^\parallel &= -r_{n2}^\parallel = \frac{\epsilon_n p - s_n}{\epsilon_n p + s_n}; \end{aligned} \tag{B6}$$

(ii) transmission coefficients for $n=1$ or 3,

$$\begin{aligned} t_{n2}^\perp &= \frac{2s_n}{p + s_n}, \\ t_{2n}^\perp &= \frac{2p}{p + s_n}, \\ t_{n2}^\parallel &= \frac{2\sqrt{\epsilon_n} s_n}{\epsilon_n p + s_n}, \\ t_{2n}^\parallel &= \frac{2\sqrt{\epsilon_n} p}{\epsilon_n p + s_n}. \end{aligned} \tag{B7}$$

It should be noted that the reflection coefficients are frequency dependent via the frequency dependent dielectric constant, $\epsilon(\omega_k)$. By expanding $1/\Delta_\lambda$ in a geometrical series, it is clear that the mode function between the two planar surfaces includes multiple reflection contributions.

APPENDIX C: CALCULATIONS OF $\tilde{F}(k)$ AND $\tilde{D}(ik)$ IN SHORT DISTANCE LIMIT

Using the mode functions, given in Appendix (B), in the planar microcavity, we calculate $\tilde{F}(k)$ first. From the definition of $\tilde{F}(k)$ given in Eq. (15) and mode function in Eq. (B1), we find

$$\tilde{F}_{\mathrm{I}}(k) = \tilde{F}_{\mathrm{I}}^{\mathrm{even}}(k) + \tilde{F}_{\mathrm{I}}^{\mathrm{odd}}(k), \tag{C1}$$

where

$$\begin{aligned} \tilde{F}_{\mathrm{I}}^{\mathrm{even}}(k) &\equiv -\frac{\omega^3}{4\pi c^3} \mathrm{Re} \int d\Omega \sum_\lambda [\hat{e}_{k\lambda}^i (\hat{e}_{k\lambda}^i)^* e^{ik_+\cdot(r_{\mathrm{A}} - r_{\mathrm{B}})} \\ &\quad + \hat{e}_{k\lambda}^r (\hat{e}_{k\lambda}^r)^* e^{ik_+\cdot(r_{\mathrm{A}} - r_{\mathrm{B}})}], \\ \tilde{F}_{\mathrm{I}}^{\mathrm{odd}}(k) &\equiv -\frac{\omega^3}{4\pi c^3} \mathrm{Re} \int d\Omega \sum_\lambda [\hat{e}_{k\lambda}^i (\hat{e}_{k\lambda}^r)^* \\ &\quad \times e^{ik_+\cdot r_{\mathrm{A}} - ik_-\cdot r_{\mathrm{B}} - 2ikd\cos\theta} \\ &\quad + \hat{e}_{k\lambda}^r (\hat{e}_{k\lambda}^i)^* e^{ik_-\cdot r_{\mathrm{A}} - ik_+\cdot r_{\mathrm{B}} + 2ikd\cos\theta}. \end{aligned} \tag{C2}$$

Here $d\Omega = \sin\theta d\theta d\phi$. The first term in Eq. (C1), $\tilde{F}_{\mathrm{I}}^{\mathrm{even}}(k)$, contains even number of reflections, whereas $\tilde{F}_{\mathrm{I}}^{\mathrm{odd}}(k)$ does odd number of reflections. This can be seen by expanding the Airy function, $1/|\Delta_\lambda|^2$, as a geometrical series. In the following derivation we assume $z_{\mathrm{A}} > z_{\mathrm{B}}$. Inserting the polarization vectors listed in Eqs. (D3) into Eq. (C2) and evaluating integrals over ϕ, we find, after some algebra,

$$\begin{aligned} \tilde{F}_{\mathrm{I}}^{\mathrm{even}}(k) &= \frac{\omega^3}{2c^3} \mathrm{Re} \int_\Gamma dp \Bigg(\frac{|t_{12}^\parallel|^2}{|\Delta_\parallel|^2} (1 + |r_{23}^\parallel|^2) \Bigg\{ \tilde{I} \Bigg[f(u) \\ &\quad + \frac{1}{u} \frac{df(u)}{du} \Bigg] - \hat{r}\hat{r} \Bigg[\frac{1}{u} \frac{df(u)}{du} - \frac{d^2 f(u)}{du^2} \Bigg] \Bigg\} \\ &\quad + \frac{1}{2} \Bigg[\frac{|t_{12}^\perp|^2}{|\Delta_\perp|^2} (1 + |r_{23}^\perp|^2) - \frac{|t_{12}^\parallel|^2}{|\Delta_\parallel|^2} (1 + |r_{23}^\parallel|^2) \Bigg] \\ &\quad \times \tilde{M}(\nu) \exp(ikp\cos\psi) \Bigg) \quad (\text{for } z_{\mathrm{A}} > z_{\mathrm{B}}), \\ \tilde{F}_{\mathrm{I}}^{\mathrm{odd}}(k) &= -\frac{\omega^3}{c^3} \mathrm{Re} \int_\Gamma dp \Bigg(\frac{|t_{12}^\parallel|^2 (r_{23}^\parallel)^*}{|\Delta_\parallel|^2} \Bigg\{ \tilde{I}' \Bigg[f(U) \\ &\quad + \frac{1}{U} \frac{df(U)}{dU} \Bigg] - \hat{R}_{\mathrm{I}} \hat{R}_{\mathrm{I}}' \Bigg[\frac{1}{U} \frac{df(U)}{dU} - \frac{d^2 f(U)}{dU^2} \Bigg] \Bigg\} \\ &\quad - \frac{1}{2} \Bigg[\frac{|t_{12}^\perp|^2 (r_{23}^\perp)^*}{|\Delta_\perp|^2} + \frac{|t_{12}^\parallel|^2 (r_{23}^\parallel)^*}{|\Delta_\parallel|^2} \Bigg] \tilde{M}(V) \\ &\quad \times \exp(-ikp\cos\chi) \Bigg) \quad (\text{for } z_{\mathrm{A}} > z_{\mathrm{B}}), \end{aligned} \tag{C3}$$

where the auxiliary functions are defined as

$$\begin{aligned} u &\equiv kr, \\ U &\equiv kR_{\mathrm{I}}, \\ \nu &\equiv u\sqrt{1 - p^2}\sin\psi, \\ V &\equiv U\sqrt{1 - p^2}\sin\chi, \\ f(u) &= \exp\{iup\cos\psi\} J_0(\nu), \\ f(U) &= \exp\{-iUp\cos\chi\} J_0(V), \\ \hat{R}_{\mathrm{I}}' &\equiv (\hat{R}_{\mathrm{I}}^x, \hat{R}_{\mathrm{I}}^y, -\hat{R}_{\mathrm{I}}^z), \\ \tilde{I}' &\equiv \begin{bmatrix} 1 & 0 & 0 \\ 0 & 1 & 0 \\ 0 & 0 & -1 \end{bmatrix}, \\ \tilde{M}(\alpha) &\equiv \begin{bmatrix} J_0(\alpha) + J_2(\alpha) & 0 & 0 \\ 0 & J_0(\alpha) - J_2(\alpha) & 0 \\ 0 & 0 & 0 \end{bmatrix}. \end{aligned} \tag{C4}$$

$J_n(x)$ are the nth-order Bessel functions. The vector elements of $\mathbf{r}_{\mathrm{A}}$ is denoted as $(x_{\mathrm{A}}, y_{\mathrm{A}}, z_{\mathrm{A}})$. $\hat{r}$ and $\hat{R}_{\mathrm{I}}$ are the unit vectors of $\mathbf{r} = \mathbf{r}_{\mathrm{A}} - \mathbf{r}_{\mathrm{B}}$ and $\mathbf{R}_{\mathrm{I}} = \mathbf{r}_{\mathrm{A}} - \mathbf{R}_{\mathrm{B}}^{\mathrm{I}}$, respectively. Here $\mathbf{R}_{\mathrm{B}}^{\mathrm{I}}$ is the position of the image molecule in the lower dielectric medium [see Fig. 1(b)]. In Eqs. (C3), the integration contour Γ is from 1 to 0 on the real axis of p and from 0 to $i\infty$ on the pure imaginary axis. The integration over the real axis, from

1 to 0, represents the contribution from the propagating modes with real wave vector, whereas that over the pure imaginary axis corresponds to the evanescent mode contribution to the spatial correlation function, particularly, the imaginary part of the Green function. Detailed discussions on the integration contour has been given by Lifshiftz[16] and Tikochinsky and Spruch[44] in the contexts of the vdW interactions between two macroscopic dielectric surfaces and between an atom and a dielectric surface, respectively.

Although the general expressions given in Eqs. (C3) are lengthy and cumbersome, in the short distance limit, one may find very simplified results. Here the short distance limit means that the distances between the two molecules as well as between the two surfaces are much shorter than the most important wavelength of the whole system. For instance the wavelength of the dominant electronic transition of molecules or dielectric media is order of hundreds of nanometer. Thus if the intermolecular and intersurface distance is shorter than this length scale, the short distance approximation can be invoked. In the calculation of the van der Waals interaction defined in Eq. (14) or (17), the most important wave vector is approximately equal to the inverse of intermolecular distance. In this high frequency region, the dielectric function is close to unity, so that one can make the following approximations: (i) $s_n \cong p$ for $n=1$ and 3, (ii) the Fresnel reflection and transmission coefficients defined in Eqs. (B6) and (B7) are independent on $p(=\cos\theta)$ as a consequence of the first approximation (i), finally (iii) we ignore multiple reflection contributions, i.e., the denominator $\Delta_\lambda \cong 1$ in Eqs. (C3). Particularly, the last approximation can be understood by expanding $1/\Delta_\lambda$ as a geometrical series,

$$\frac{1}{\Delta_\lambda} = 1 + \sum_{n=1}^{\infty} (r_{21}^\lambda r_{23}^\lambda)^n \exp(2inkd\cos\theta). \tag{C5}$$

Inserting this expanded form into Eq. (C3) and using the approximations (i) and (ii), we may find $\widetilde{F}(k)$ and $\widetilde{V}(k)$ are given by sums over n. If one focuses on the terms inversely proportional to the cubic of distance—here the distance represents the shortest distance that a virtual photon may travel with multiple reflections by the two surfaces—the nth term with nonzero n can be shown to be approximately equal to $1/(r+nd)^3$. Therefore, one can ignore terms with $n \geqslant 1$. This approximation means we ignore contributions from multiple (more than once) reflections in calculating $\widetilde{F}(k)$, $\widetilde{V}(k)$, and $\widetilde{\mathbf{G}}(i\kappa)$. After some algebra, we finally find that $\widetilde{\mathbf{G}}_{\mathrm{I}}(i\kappa)$, which is associated with the type I mode contributions, is given by

$$\widetilde{\mathbf{G}}_{\mathrm{I}}(i\kappa) = \widetilde{\mathbf{G}}_{\mathrm{I}}^{\mathrm{even}}(i\kappa) + \widetilde{\mathbf{G}}_{\mathrm{I}}^{\mathrm{odd}}(i\kappa), \tag{C6}$$

where

$$\widetilde{\mathbf{G}}_{\mathrm{I}}^{\mathrm{even}}(i\kappa) \cong \frac{1}{2}\left[\frac{2\sqrt{\epsilon_1(i\kappa)}}{\epsilon_1(i\kappa)+1}\right]^2 \left\{1 + \left[\frac{\epsilon_3(i\kappa)-1}{\epsilon_3(i\kappa)+1}\right]^2\right\} \frac{\widetilde{I} - 3\hat{r}\hat{r}}{r^3},$$

$$\widetilde{\mathbf{G}}_{\mathrm{I}}^{\mathrm{odd}}(i\kappa) \cong -\left[\frac{2\sqrt{\epsilon_1(i\kappa)}}{\epsilon_1(i\kappa)+1}\right]^2 \left[\frac{\epsilon_3(i\kappa)-1}{\epsilon_3(i\kappa)+1}\right] \frac{\widetilde{I}' - 3\hat{R}_{\mathrm{I}}\hat{R}_{\mathrm{I}}'}{R_{\mathrm{I}}^3}. \tag{C7}$$

Also one can immediately find that the corresponding tensors associated with the type II modes are

$$\widetilde{\mathbf{G}}_{\mathrm{II}}^{\mathrm{even}}(i\kappa) \cong \frac{1}{2}\left[\frac{2\sqrt{\epsilon_3(i\kappa)}}{\epsilon_3(i\kappa)+1}\right]^2 \left\{1 + \left[\frac{\epsilon_1(i\kappa)-1}{\epsilon_1(i\kappa)+1}\right]^2\right\} \frac{\widetilde{I} - 3\hat{r}\hat{r}}{r^3},$$

$$\widetilde{\mathbf{G}}_{\mathrm{II}}^{\mathrm{odd}}(i\kappa) \cong -\left[\frac{2\sqrt{\epsilon_3(i\kappa)}}{\epsilon_3(i\kappa)+1}\right]^2 \left[\frac{\epsilon_1(i\kappa)-1}{\epsilon_1(i\kappa)+1}\right] \frac{\widetilde{I}' - 3\hat{R}_{\mathrm{II}}\hat{R}_{\mathrm{II}}'}{R_{\mathrm{II}}^3}. \tag{C8}$$

Equations (C7) and (C8) are the main results, Eq. (21), used in Sec. III.

[1] *Advances in Atomic, Molecular, and Optical Physics; Cavity Quantum Electrodynamics, Suppl. 2* (Academic, New York, 1994).
[2] R. R. Chance, A. Prock, and R. J. Silbey, Adv. Chem. Phys. **37**, 1 (1978), and references therein.
[3] G. W. Ford and W. H. Weber, Phys. Rep. **113**, 195 (1984).
[4] R. Loudon, *The Quantum Theory of Light*, 2nd ed. (Oxford University, Oxford, 1983).
[5] P. W. Milonni, *The Quantum Vacuum, An Introduction to Quantum Electrodynamics* (Academic, New York, 1994).
[6] H. Khosravi and R. Loudon, Proc. R. Soc. London, Ser. A **433**, 337 (1991); **436**, 373 (1992).
[7] R. Glauber and M. Lewenstein, Phys. Rev. A **43**, 467 (1991).
[8] A. D. McLachlan, Mol. Phys. **7**, 381 (1964).
[9] H. Imura and K. Okano, J. Chem. Phys. **58**, 2763 (1973).
[10] R. G. Horn and J. N. Israelachvili, J. Chem. Phys. **75**, 1400 (1981).
[11] J. N. Israelachvili, P. M. McGuiggan, and A. M. Homola, Science **240**, 189 (1988); M. Schoen, C. L. Rhykerd, Jr., D. J. Diestler, and J. H. Cushman, *ibid.* **245**, 1223 (1989); P. A. Thompson and M. O. Robbins, *ibid.* **250**, 792 (1990); S. Granick, *ibid.* **253**, 1374 (1991).
[12] J. Klein and E. Kumacheva, Science **269**, 816 (1995).
[13] F. P. Bowen and D. Tabor, *Friction and Lubrication* (Oxford University, Oxford, 1958); E. Rabinowicz, *Friction and Wear of Materials* (Wiley, New York, 1965).
[14] F. M. Etzler and W. Prost-Hansen, Adv. Chem. Ser. **188**, 486 (1980).
[15] H. K. Christenson, D. W. R. Gruen, R. G. Horn, and J. N. Israelachvili, J. Chem. Phys. **87**, 1834 (1987).
[16] (a) E. M. Lifshitz, Sov. Phys. JETP **2**, 73 (1956); (b) I. E. Dyzaloshinskii, E. M. Lifshitz, and L. P. Pitaevskii, Adv. Phys. **10**, 165 (1961).
[17] A. Zangwill, *Physics at Surfaces* (Cambridge University, Cambridge, 1988).
[18] N. D. Lang and W. Kohn, Phys. Rev. B **1**, 4555 (1970).
[19] G. Mukhopadhyay and S. Lundqvist, Phys. Scr. **17**, 69 (1978).
[20] K. L. Kliewer, Surf. Sci. **101**, 57 (1980).
[21] P. J. Feibelman, Phys. Rev. Lett. **34**, 1092 (1975).
[22] T. Maniv and H. Metiu, J. Chem. Phys. **76**, 2697 (1982).
[23] E. Zaremba and W. Kohn, Phys. Rev. B **13**, 2270 (1976).
[24] C. Cohen-Tannoudji, J. Dupont-Roc, and G. Grynberg, *Photons and Atoms, Introduction to Quantum Electrodynamics* (Wiley–Interscience, New York, 1989).
[25] E. A. Power and S. Zienau, Philos. Trans. R. Soc. London, Ser. A **251**, 427 (1959).
[26] D. P. Craig and T. Thirunamachandran, *Molecular Quantum Electrodynamics, An Introduction to Quantum Electrodynamics* (Academic, London, 1984).
[27] L. Spruch and E. J. Kelsey, Phys. Rev. A **18**, 845 (1978).
[28] P. W. Milonni and M.-L. Shi, Phys. Rev. A **45**, 4241 (1992).
[29] F. London, Z. Phys. **63**, 245 (1930); Z. Phys. Chem B **11**, 222 (1930); J. E. Lennard-Jones, Trans. Faraday Soc. **28**, 334 (1932).
[30] W. Heitler, *The Quantum Theory of Radiation*, 3rd ed. (Clarendon, Oxford, 1954).
[31] E. A. Power and T. Thirunamachandran, Phys. Rev. A **48**, 4761 (1993).
[32] R. R. McLone and E. A. Power, Mathematika **11**, 91 (1965).
[33] E. M. Lifshitz and L. P. Pitaevskii, *Statistical Physics. Part 2, Theory of the Condensed State* (Pergamon, New York, 1980).
[34] Yu. S. Barash and V. L. Ginzburg, Sov. Phys. Usp. **27**, 467 (1984).
[35] J. Unguris, L. W. Bruch, E. R. Moog, and M. B. Webb, Surf. Sci. **87**, 415 (1979).
[36] L. W. Bruch, J. Unguris, and M. B. Webb, Surf. Sci. **87**, 437 (1979).
[37] L. W. Bruch, Surf. Sci. **125**, 194 (1983).

[38] S. Rauber, J. Klein, and M. Cole, Phys. Rev. B **27**, 1314 (1983).
[39] L. D. Landau and E. M. Lifshitz, *Electrodynamics of Continuous Media* (Pergamon, Oxford, 1960).
[40] G. D. Mahan, *Many-Particle Physics* (Plenum, New York, 1981).
[41] M. Cho and R. J. Silbey, Chem. Phys. Lett. **242**, 291 (1995).
[42] F. De Martini, M. Marrocco, P. Mataloni, L. Crescentini, and R. Loudon, Phys. Rev. A **43**, 2480 (1991); F. De Martini, M. Marrocco, P. Mataloni, D. Murra, and R. Loudon, J. Opt. Soc. Am. B **10**, 360 (1993).
[43] M. Born and E. Wolf, *Principles of Optics* (Pergamon, Oxford, 1970).
[44] Y. Tikochinsky and L. Spruch, Phys. Rev. A **48**, 4223 (1993).